Acta Oceanol. Sin., 2024, Vol. 43, No. 8, P. 26–36
https://doi.org/10.1007/s13131-024-2335-6
http://www.aosocean.com
E-mail: ocean2@hyxb.org.cn

Geochemical characteristics and origins of natural gases in the eastern Cote d'Ivoire Basin, West Africa

Li Li[1, 2*], Quan Li[1], Tao Cheng[1], Songling Yang[1], Yong Rao[1], Xinyu Liu[1], Wenjing Ding[2, 3]

[1] CNOOC International Ltd., Beijing 100028, China

[2] School of Natural Sciences, Macquarie University, Sydney, NSW, 2109, Australia

[3] CNOOC Research Institute, Beijing 100028, China

Received 23 July 2023; accepted 5 December 2023

Abstract

The gas sources in the eastern Cote d'Ivoire Basin (Tano Basin) are seldom reported and remain controversial due to multiple sets of potential source rocks and poorly documented geochemical characteristics of natural gases. The marine source rock potential from the Upper Albian to Turonian as well as the molecular composition and the stable carbon isotope composition of natural gases in the eastern Cote d'Ivoire Basin were studied in detail to investigate the origins of natural gases. The total organic carbon (TOC), hydrogen index (HI), and generation potential ($S_1 + S_2$) of source rocks indicate that both sapropelic source rocks and humic source rocks developed during the late Albian, whereas sapropelic source rocks developed during the Cenomanian and the Turonian. The normal order of $\delta^{13}CH_4 < \delta^{13}C_2H_6 < \delta^{13}C_3H_8$ ($\delta^{13}C_1 < \delta^{13}C_2 < \delta^{13}C_3$), the relationship between C_2/C_3 molar ratio and $\delta^{13}C_2$-$\delta^{13}C_3$, and the plot of $\delta^{13}C_1$ versus $C_1/(C_2+C_3)$ collectively show that the natural gases are thermogenic due to the primary cracking of kerogen, including the typical oil-associated gases from Well D-1, the mixed oil-associated gases and coal-derived gases from Well G-1 and Well L-1. Based on the plot of $\delta^{13}C_1$ versus $\delta^{13}C_2$ and the established relationship between $\delta^{13}C_1$ and equivalent vitrinite reflectance (Ro), we proposed that the natural gases are in a mature stage (Ro generally varies from 1.0% to 1.3%). Combined with results of basin modelling and oil-to-source correlation, the transitional to marine source rocks during the late Albian were thought to have made a great contribution to the natural gases. Our study will make a better understanding on petroleum system in the eastern Cote d'Ivoire Basin.

Key words: marine source rocks potential, molecular composition, stable carbon isotopes, Upper Albian, Tano Basin

Citation: Li Li, Li Quan, Cheng Tao, Yang Songling, Rao Yong, Liu Xinyu, Ding Wenjing. 2024. Geochemical characteristics and origins of natural gases in the eastern Cote d'Ivoire Basin, West Africa. Acta Oceanologica Sinica, 43(8): 26–36, doi: 10.1007/s13131-024-2335-6

1 Introduction

The hydrocarbon exploration in the Cote d'Ivoire Basin began in the late 19th century, and a total of 81 discoveries that range from non-commercial to large have been made in this basin (Lake et al., 2014; Bempong et al., 2019). In the early stages of exploration, the use of seismic data resulted in some non-commercial discoveries. After 2000, the exploration shifted to deep water. The major commercial oil discovery in the mahogany prospect of the West Cape Three Points License formed the Jubilee field with 916 MMboe of recoverable reserves, resulting in the first exploration boom in the Basin (Bempong et al., 2019). In the past five years, the commercial discoveries of the Afina field in 2019 (354 MMboe of recoverable reserves), the Eban field in 2021 (117 MMboe of recoverable reserves), and the Baleine field in 2021 (780 MMboe of recoverable reserves) have set off another oil and gas exploration boom.

As a whole, it still has great petroleum exploration potential in terms of highly prospective discovered reserves (Morrison et al., 2000; Bird et al., 2001; Rüpke et al., 2010; Dailly et al., 2013; Davison et al., 2016; Tetteh, 2016; Bempong et al., 2019). The eastern Cote d'Ivoire Basin, also known as the Tano Basin, is recognized as the eastern extension of Cote d'Ivoire and Ghana (Bempong et al., 2019). It covers an area of about 3 000 km^2 and occupies largely offshore and less onshore segments in the southwestern part of Ghana. In recent years, several new-field wildcat wells, including Well D-1, Well L-1, and Well G-1, were drilled and encountered significant thickness of gas and condensate sands, confirming its rich natural gas resources. Source rocks of the Cote d'Ivoire Basin are restricted to Cretaceous age (Strand, 1998; Bird et al., 2001). However, the properties of lacustrine source rocks spanning through the Aptian to Lower Albian are largely unavailable and unknown due to their large burial depths. The marine source rocks from the Upper Albian to Turonian have been penetrated suggesting rich oil-prone source potential (Atta-Peters and Garrey, 2014; Atta-Peters et al., 2015; Garry et al., 2016; Bempong et al., 2019). As important source rock interval, the Albian series were deposited in environments grading from lacustrine to marine, allowing the preservation of both oil-prone source rocks and gas-prone source rocks (Chierici, 1996; Benkhelil et al., 1998; Lake et al., 2014). The gas source is seldomly reported and re-

Foundation item: The Major Science and Technology Project of CNOOC under contract No. KJGG2022-0902; the National Natural Science Foundation of China under contract Nos 42202184 and 42272177.
*Corresponding author, E-mail: li.li40@hdr.mq.edu.au

mains controversial due to multiple sets of potential source rocks and the poorly investigated geochemical characteristics of natural gases. This will hinder the understanding on formation and accumulation of natural gases in the eastern Cote d'Ivoire Basin.

In natural gas geochemistry, molecular and stable carbon isotope compositions of gaseous alkanes contain ample information on geologic backgrounds (organic source, sedimentary environment) and geochemical processes during hydrocarbon generation. In order to assessing natural gas resource potential and finding favorable areas for exploration, many researchers have established numerous parameters and classic diagrams to shed insights into deciphering the formation of natural gases (Berner et al., 1992; Dai, 1992; Prinzhofer and Battani, 2003; Dai et al., 2005, 2016; Milkov and Etiope, 2018; Milkov, 2018; Li et al., 2022). The correlation between chemical compositions and isotopes are regarded as important diagnostic tools for assessment of its sources and exploration potential.

In this study, cores and natural gases from three wells (Well D-1, Well L-1, and Well G-1) were sampled and analyzed to investigate their geochemical characteristics and gas-source correlation. The source rock potential was discussed based on the analyses of the total organic content and Rock-Eval pyrolysis. The genetic types and thermal maturity of natural gases were revealed by their characteristics of molecular components and stable carbon isotope compositions. This study will be beneficial for better understanding on the main source of natural gases and it will be a guide to the future natural gas exploration in the eastern Cote d' Ivoire Basin.

2 Geological setting

The eastern Cote d'Ivoire Basin, also known as the Tano Basin, is an east-west orientated sedimentary basin. It is located on the south coast of Ghana and extends to the southeast coast of Cote d'Ivoire (Fig. 1). It is a typical transform margin basin that is bounded respectively by the Saint Paul Fracture Zone to the east and the Romanche Fracture Zone to the west. This basin has undergone a complex tectonic history and formed as a result of the break-up of Gondwanaland (Mascle and Blarez, 1987; Blarez and Mascle, 1988; Basile et al., 1993, 1998; Clift et al., 1997; Lake et al., 2014; Ye et al., 2019). This basin began rifting in the Aptian (or the Barremian), resulting in the deposition of lacustrine sediments. With the south Atlantic opened from south to north, the continental separation and the rift-to-drift transition probably occurred during the late Albian to Cenomanian, resulting in the development of the lacustrine sequence overlain by the restricted-marine and the subsequent open-marine sequences (Chierici, 1996; Lake et al., 2014; Ye et al., 2019). A series of the early Cretaceous pull-apart depocenters is bounded by extensional faults associated with the Saint Paul Transform Fault to the northwest. These depocenters are subdivided by large transpressional arches associated with the Romanche transform movement to the southeast.

The early source rocks are organic-rich lacustrine sediments that developed within the Aptian-early Albian. The distribution of the lacustrine source rocks was influenced strongly by rift tectonic activity (Antobreh et al., 2009). Then, the separation of Africa from South America that started from the Late Albian caused the development of the transitional-to-marine source

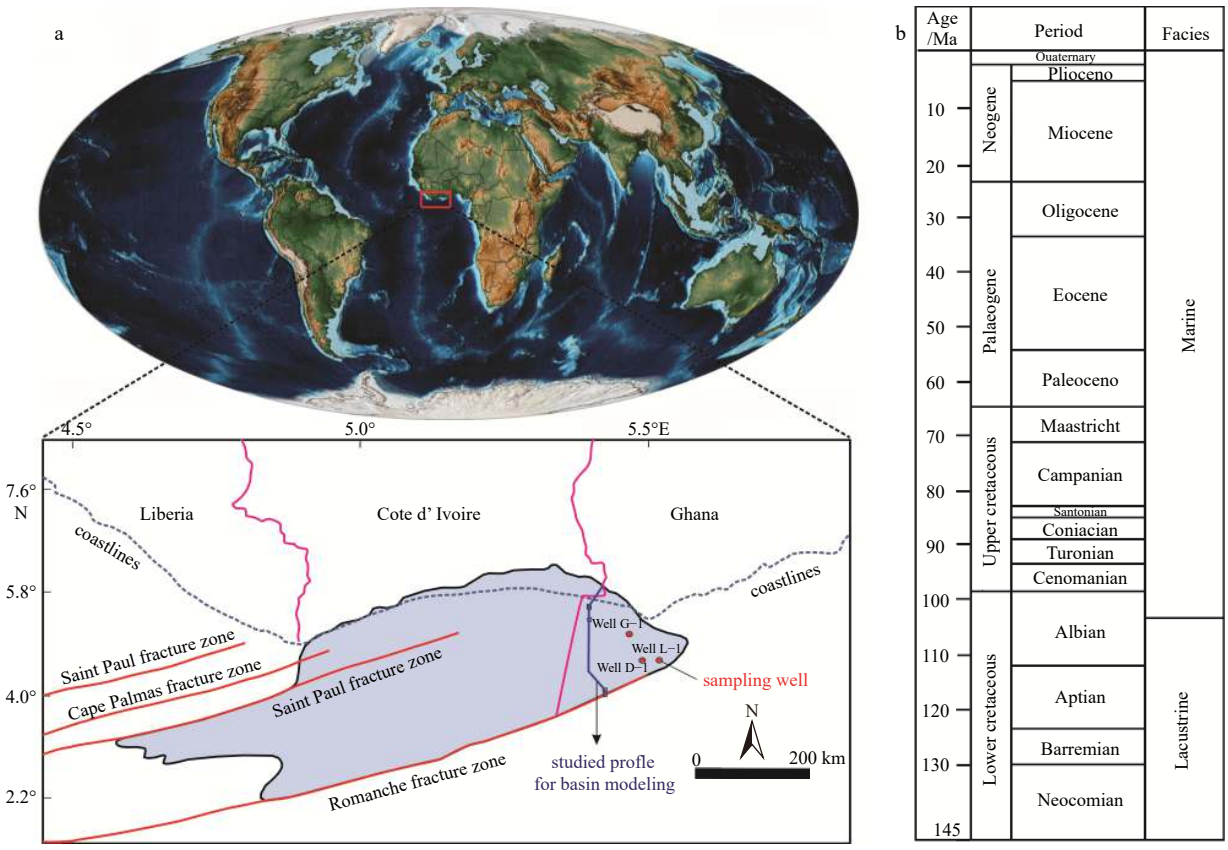

Fig. 1. Simplified structural map of the Cote d'Ivoire Basin and distributions of the three sampled wells in the basin (a). Stratigraphic table of the major Cretaceous strata in the Cote d'Ivoire Basin (modified from Morrison et al., 2000) (b).

rocks. It is proposed that the formation of organic-rich marine source rocks is greatly influenced by marine transgression and global oceanic anoxic events (Wagner, 2002; Lake et al., 2014). Based on oil geochemistry and source rocks maturity data, it is suggested that the Albian and Cenomanian-Turonian series contain the main source rocks in this basin (Morrison et al., 2000; Rüpke et al., 2010; Lake et al., 2014). Abundant hydrocarbons, discovered varying in age from the Albian to Campanian, have proved the resource potential both in the Lower and Upper Cretaceous clastic reservoirs (Bird et al., 2001; Brownfield and Charpentier, 2006; Dailly et al., 2013; Davison et al., 2016).

3 Samples and methods

Emphasis is given to the Albian-Turonian source rock samples, because the younger shales are generally in immature thermal stage, even within basinal depocentres. Source rocks potential analyses [total organic carbon (TOC, %wt.), Rock-Eval pyrolysis], molecular composition analysis and stable carbon isotope composition analysis of natural gases were carried out. The locations of the three sampled wells (Well G-1, Well L-1, and Well D-1) in the eastern Cote d'Ivoire Basin are present in Figure 1. The results of the analyses are shown in Table 1 and Table 2.

Table 1. Total organic carbon (TOC, %wt.) content, Rock-Eval pyrolysis and vitrinite reflectance (Ro, %) from source rocks in the eastern Cote d'Ivoire Basin

Well	Formation	TOC/%			$S_1 + S_2$ (HC/Rock)			HI (HC/TOC)			T_{max} /℃		
		Min.	Max.	Average	Min.	Max.	Average	Min.	Max.	Average	Min.	Max.	Average
G-1	Turonian	1.38	2.48	1.92	3.8	21.36	9.01	207	888	453	405	437	433
	Cenomanian	1.63	1.99	1.88	5.72	7.32	6.83	334	369	356	435	438	436
	Albian	0.54	1.24	0.89	0.95	4.96	2.26	144	391	235	432	440	437
L-1	Turonian	1.43	3.08	2.04	6.69	19.1	10.78	441	614	518	426	434	430
	Cenomanian	0.54	2.97	1.42	1.54	18.47	6.91	275	676	444	431	436	434
	Albian	0.51	0.72	0.59	0.37	0.74	0.57	49	111	81	425	443	437
D-1	Turonian	2.29	3.22	2.62	12.14	21.04	15.49	498	674	586	412	422	418
	Cenomanian	1.67	4.06	2.91	7.83	28.94	18.55	442	712	606	417	424	420
	Albian	0.74	1.72	1.25	1.00	6.67	4.02	74	500	228	425	441	435

Note: Ro: vitrinite reflectance; TOC: total organic carbon concentration; S_1 = free hydrocarbons yield; S_2 = pyrolytic hydrocarbon yield; $S_1 + S_2$ = generation potential; HI: hydrogen index = $S_2 \times 100$/TOC; T_{max} = temperature of maximum generation.

Table 2. Molecular component molar ratio (%) and stable carbon isotopic composition (‰, V_{PDB}) from natural gases in the eastern Cote d'Ivoire Basin

Well	Main molecular composition molar ratio/%				Carbon isotope/‰		
	CH_4	C_2H_6	C_3H_8	C_4H_{10}	δ^{13}C-CH_4	δ^{13}C-C_2H_6	δ^{13}C-C_3H_8
G-1	60.8	17.7	12.4	3.2	–33.5	–27.0	–26.9
	69.1	17.2	9.1	3.4	–33.6	–27.5	–27.8
	68.6	17.9	8.4	3.2	–32.3	–27.3	–27.4
L-1	71.4	15.4	9.7	2.9	–35.0	–29.4	–28.3
	68.8	15.0	10.9	4.0	–33.4	–26.2	–25.0
	76.5	13.2	7.0	2.5	–34.8	–29.8	–27.9
	71.7	17.2	8.0	2.4	–31.7	–29.5	–27.6
	70.7	17.6	8.2	2.5	–31.7	–29.6	–27.8
	71.6	17.5	7.9	2.3	–31.9	–29.7	–28.0
	71.4	17.7	7.9	2.2	–31.0	–29.2	–27.7
	71.7	18.0	7.6	2.0	–31.9	–28.3	–27.7
	75.8	15.5	6.2	1.8	–33.7	–28.7	–27.9
	75.4	15.4	6.7	1.9	–32.2	–26.9	–26.7
	70.7	19.4	7.6	1.8	–31.2	–28.2	–27.3
	76.8	16.6	5.3	1.1	–32.0	–28.4	–27.3
	69.4	21.1	7.5	1.7	–33.2	–29.7	–28.2
	69.7	20.8	7.5	1.6	–31.4	–29.1	–28.1
	70.1	17.0	9.1	3.0	–31.0	–26.3	–26.3
	76.8	15.9	5.8	1.3	–31.9	–28.4	–28.0
	70.6	19.2	8.0	1.8	–29.9	–27.7	–27.6
	75.8	15.6	6.4	1.7	–30.9	–27.2	–26.9
D-1	84.6	7.3	4.3	2.1	–41.8	–29.9	–28.5
	85.0	7.5	3.8	1.9	–41.6	–30.2	–28.5
	85.4	7.4	3.6	1.8	–40.8	–30.1	–28.7
	86.1	7.4	3.5	1.6	–41.5	–30.6	–28.7
	85.4	7.5	3.7	1.8	–41.7	–30.3	–28.9
	77.4	9.7	5.8	3.4	–41.7	–30.8	–29.2

Before analysis for TOC and Rock-Eval pyrolysis, a total of 230 isojar cuttings samples from the Upper Albian-Turonian of three wells were extracted sequentially with dichloromethane to remove contaminants from the drill cuttings. Then these cuttings were crushed to a size of ⩽0.075 mm. Around 70 mg of each powdered sample were pre-treated with concentrated HCl and rinsed with deionized water for more than 50 times, then analysed for TOC analysis using a Leco elemental analyser. About 50 mg of each powdered samples were analysed for Rock-Eval analysis using a Delsi Rock-Eval RE Ⅱ instrument (Espitalié et al., 1984). An external standard was used every ten samples to ensure the quality of the TOC analysis and Rock-Eval pyrolysis analysis.

A total of 27 headspace gas (isojar) samples from the Upper Albian reservoirs of three wells were collected for both gas component analysis and stable carbon isotope component analysis by standard methods in Hill et al. (2007). Gas component of C_1–C_5 was analyzed in triplicate using a Hewlett Packard 6890 series gas chromatogragh equipped with a flame ionization detector. Stable carbon isotopes of C_1–C_3 was measured by a Micromass Optima mass spectrometer interfaced with a Hewlett Packard 6890 series gas chromatogragh. The stable carbon isotopic values are within the precision of ±0.3‰ and subject to the Vienna PeeDee Belemnite (V_{PDB}) standard.

4 Results

4.1 *Source rocks potential*

There appears to be a decrease in source potential towards the Upper Albian in the locations of three sampled wells. The values of TOC and $S_1 + S_2$ of source rocks from the Cenomanian-Turonian is generally higher than that from the Albian (Table 1, Fig. 2a): (1) For the Upper Albian source rocks: Well G-1, TOC average 0.89%; $S_1 + S_2$ average 2.26 mg/g; Well L-1, TOC average 0.59%; $S_1 + S_2$ average 0.57 mg/g; Well D-1, TOC average 1.25%; $S_1 + S_2$ average 4.02 mg/g. (2) For the Cenomanian source rocks: Well G-1, TOC average 1.88%; $S_1 + S_2$ average 6.83 mg/g (HC/Rock); Well L-1, TOC average 1.42%; $S_1 + S_2$ average 6.91 mg/g (HC/Rock); Well D-1, TOC average 2.91%; $S_1 + S_2$ average 18.55 mg/g (HC/Rock). For the Turonian source rocks: Well G-1, TOC average 1.92%; $S_1 + S_2$ average 9.01 mg/g (HC/Rock); Well L-1, TOC average 2.04%; $S_1 + S_2$ average 10.78 mg/g (HC/Rock); Well D-1, TOC average 2.62%; $S_1 + S_2$ average 15.49 mg/g (HC/Rock). Therefore, the TOC together with the $S_1 + S_2$ reflect a higher hydrocarbon generation potential of the Cenomanian-Turonian source rocks (Fig. 2a) than the Upper Albian source rocks. The Upper Albian source rocks generally have lower hydrogen index (HI) values (average 235 mg/g (HC/TOC) from Well G-1, average 81 mg/g (HC/TOC) from Well L-1, and average 228 mg/g (HC/TOC) from Well D-1) than the Cenomanian-Turonian source rocks. This is likely influenced by the higher thermal maturity of the Upper Albian source rocks, with their average T_{max} (435–437℃) higher than the Cenomanian-Turonian source rocks (average T_{max} in 418–436℃). However, the cross-plot of T_{max} versus HI indicates a dominant type Ⅲ–Ⅱ$_2$ kerogens in the Upper Albian samples and a dominant type Ⅱ$_2$–Ⅱ$_1$ kerogens in the Cenomanian-Turonian samples (Fig. 2b). This implies a predominantly terrigenous contribution to the Upper Albian organic matter. Thus, the Upper Albian source rocks are characterised by more gas-prone compared to the Cenomanian-Turonian source rocks.

4.2 *Molecular and stable carbon isotope compositions of natural gases*

The main molecular composition and stable carbon isotope composition of the natural gases from the Upper Albian sandstone reservoirs in the eastern Cote d'Ivoire are presented in Table 2.

Among all the measured hydrocarbon gases, methane (C_1) contents vary from 60.8% to 86.1% (average 74.3%), ethane (C_2) contents vary from 7.3% to 21.1% (average 15.1%), and propane (C_3) contents vary from 3.5% to 12.4% (average 7.1%), butane (C_4)

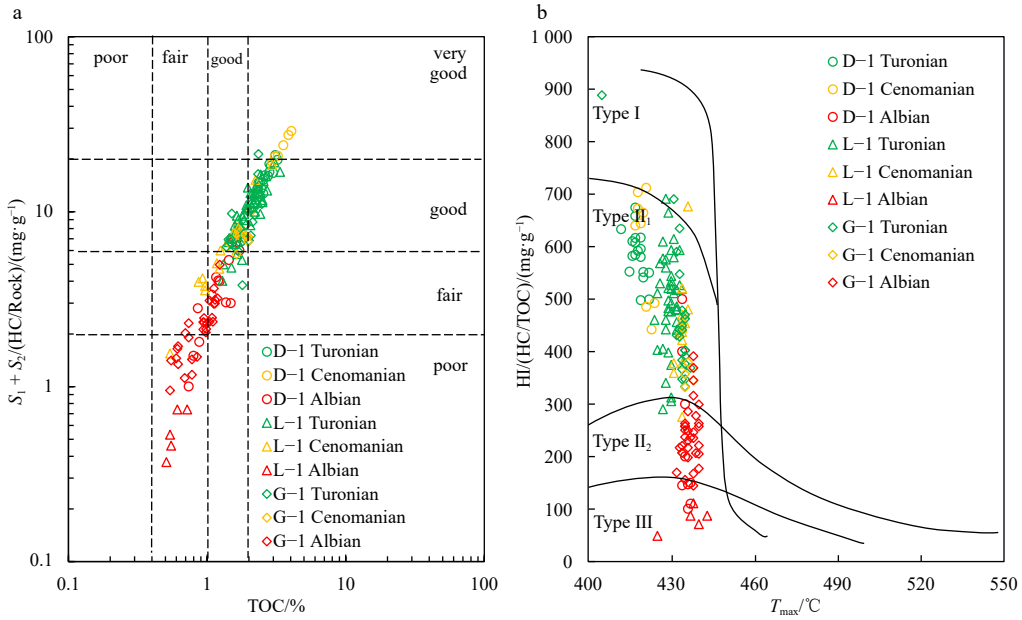

Fig. 2. Plot of total organic carbon (TOC) versus generated hydrocarbons ($S_1 + S_2$) showing source rock quality (a). Plot of hydrogen index (HI) versus maximum hydrocarbon generation (T_{max}) showing kerogen types (refer to Espitalié et al., 1984) (b). HI = S_2/total organic carbon × 100.

contents vary from 1.05% to 4.04% (average 2.3%). Natural gas dryness $C_1/(C_2+C_3)$ of the samples ranges from 2.02 to 7.92 with an average of 3.84%. The drying coefficient ($C_1/\Sigma C_{1-4}$) of the samples is between 0.65 and 0.87 (average 0.75). C_1 contents of the samples of Well D-1 (77.4%–86.1%) are higher than that of the other two wells (0.61–0.77), resulting in their higher $C_1/(C_2+C_3)$ ratios and $C_1/\Sigma C_{1-4}$ ratios.

The stable carbon isotopes of the natural gases appear in a positive order ($\delta^{13}C_1 < \delta^{13}C_2 < \delta^{13}C_3$) (Fig. 3). The $\delta^{13}C_1$ values are the highest among the gas composition, ranging from –41.8‰ to –29.9‰, with an average value of –34.3‰. The $\delta^{13}C_1$ values of the natural gases from Well D-1 are higher than that from the other two wells. The $\delta^{13}C_2$ and $\delta^{13}C_3$ values vary from –30.8‰ to –26.2‰ (average –28.7‰), and from –29.2‰ to –25.0‰ (average 27.7‰), respectively.

5 Discussion

5.1 *Genetic types of natural gases*

Based on two distinct generation mechanisms, natural gases can be divided into inorganic gases and organic gases (Dai, 1992). The latter can further be divided into biogenic, mixed genetic, and thermogenic gases according to their different formation processes. The molecular composition characteristics and stable carbon isotope values of gaseous alkanes in natural gases can be used for genetic type classification of organic gases (Dai et al., 1987; Berner et al., 1992; Dai, 1992; Prinzhofer and Huc, 1995; Dai et al., 2016; Faramawy et al., 2016; Milkov and Etiope, 2018). Inorganic gases are generally characterised by negative carbon isotope series (i.e., $\delta^{13}C_1 > \delta^{13}C_2 > \delta^{13}C_3 > \delta^{13}C_4$), and $\delta^{13}C_1$ values are high (generally between –30‰ and –10‰). By contrast, organic gases generally have positive carbon isotope series (i.e., $\delta^{13}C_1 < \delta^{13}C_2 < \delta^{13}C_3 < \delta^{13}C_4$), whereas reversed trends are caused by different mixing processes of different gentic types and thermal maturity of organic gases (Dai, 1992; Dai et al., 2008). The dryness [$C_1/(C_2+C_3)$ ratio] of biogenic gases is commonly higher than that of thermogenic gases, and they have lower $\delta^{13}C_1$ values (generally < 55‰) (Bernard et al., 1976; Faber and Stahl, 1984; Whiticar and Suess, 1990; Milkov and Etiope, 2018). Thermogenic gases are classified into sapropelic-type (or oil-type) and humic-type (or coal-derived) gases. Since thermal maturity has limited impact on $\delta^{13}C_2$ of parent gas source rocks,

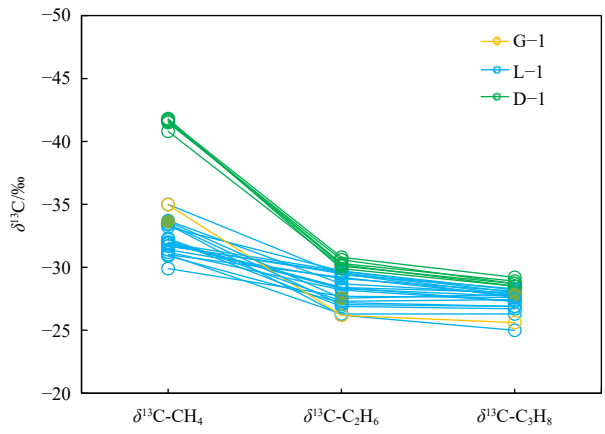

Fig. 3. The stable carbon isotopes distribution of gaseous alkanes (methane CH_4, ethane C_2H_6, and propane C_3H_8) in the eastern Cote d'Ivoire Basin.

$\delta^{13}C_2$ value of thermogenic gases has been widely used to distinguish oil-type and coal-derived gases (Dai, 1992; Berner and Faber, 1996; Dai et al., 2005; Li et al., 2022; Huang et al., 2015; Wang et al., 2015). The $\delta^{13}C_2$ value of –27‰ and –29‰ can be used as the boundary of the coal-type and oil-derived gases (Dai et al., 2005; Li et al., 2022). Specially, oil-type gases generally have lower $\delta^{13}C_2$ values (commonly $\delta^{13}C_2 < -29‰$) than coal-derived (commonly $\delta^{13}C_2 > -27‰$), and $\delta^{13}C_2$ values between –29‰ and –27‰ often reflect a mixture of these two types of gases. However, some studies also proposed that the $\delta^{13}C_2$ threshold may not be reliable when identifying genetic types of thermogenic gases if these gases originate from multiple sets of source rocks or are influenced by microbial oxidation and diffusive fractionation (Dai, 1992; Prinzhofer and Huc, 1995; Prinzhofer and Pernaton, 1997; Dai et al., 2016). Therefore, when using carbon isotope compositions to identify the genesis of natural gases, it is necessary to consider the existence of different mixing processes.

In this study, several cross-plots of molecular composition and stable carbon isotopes of natural gases were used to identify the genetic types of natural gases in the eastern Cote d'Ivoire Basin. The normal order of $\delta^{13}C_1 < \delta^{13}C_2 < \delta^{13}C_3$ and the $\delta^{13}C_1$ values of greater than –55‰ reflect that the natural gases are organic origin (Table 2; Fig. 3). Various gas origins including oil-type gases, coal-derived gases, and a mixture of oil- and coal-derived gases were observed in the discrimination graph of $\delta^{13}C_1$-$\delta^{13}C_2$-$\delta^{13}C_3$ (Fig. 4) (Dai, 1992; Dai et al., 2014). The relationship between C_2/C_3 molar ratio and $\delta^{13}C_2$-$\delta^{13}C_3$ shows that the natural gases are derived from the primary cracking of kerogen, with limited variance of C_2/C_3 molar ratio (1.38–3.11, average 2.15) (Fig. 5) (Prinzhofer et al., 2000; Prinzhofer and Battani, 2003). In the revised "Bernard plot" [plot of $\delta^{13}C_1$ versus $C_1/(C_2+C_3)$] (Milkov, 2018) (Fig. 6), all gas samples are distributed in the area of thermogenic gas and in the junction areas of abiotic gas, far away from the primary microbial area. Different relationships of $\delta^{13}C_1$ versus $C_1/(C_2+C_3)$ between thermogenic and biogenic gases were observed by Dai (1992). The gas samples fall in the thermogenic gas area, with the low $C_1/(C_2+C_3)$ ratios of less than 50 (Fig. 7). Therefore, the natural gases are all thermogenic and not subjected to microbial oxidation processes. Compared to the typical oil-associated gas samples from Well D-1, the mixed oil-associated gases and coal-derived gases of Well G-1 and Well L-1 were indicated by the higher $\delta^{13}C_1$ values (Fig. 7). Some gas samples of Well L-1 plot in the coal-derived gas zone. To conclude, combined with the cross-plots mentioned above (Figs 4, 5, 6 and 7), these natural gases from the primary cracking of kerogen were classified into two groups: oil-type gases from Well D-1; a mixed oil-type gases and coal-derived gases from Well G-1 and Well L-1.

5.2 *Thermal maturity of natural gases*

Although stable carbon isotopes of natural gases are generally inherited from kerogens, they are also influenced by thermal maturity in various degrees and will become heavier with increasing thermal maturity (Berner et al., 1992; Rooney et al., 1995; Berner and Faber, 1996; Su et al., 2018). Compared to $\delta^{13}C_2$, thermal evolution has a greater influence on $\delta^{13}C_1$ (Dai, 1992). $\delta^{13}C_1$ values of oil-type gases that are derived from sapropelic organic matter exhibit a greater control on thermal maturity than organic sources. Synthesizing genetic type and thermal evolution, the thermal maturity evaluation of natural gas using the plot of $\delta^{13}C_1$ versus $\delta^{13}C_2$ was established by Li et al. (2022).

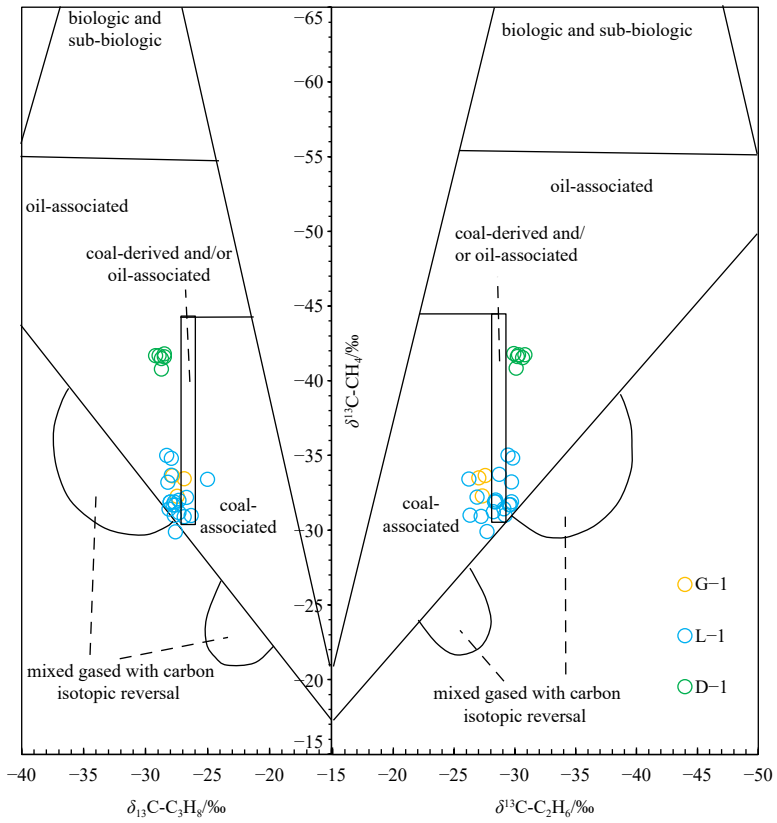

Fig. 4. The origin of natural gas interpretative diagram based on δ^{13}C-CH$_4$, δ^{13}C-C$_2$H$_6$, and δ^{13}C-C$_3$H$_8$ data in the eastern Cote d'Ivoire Basin (refer to Dai et al., 2014).

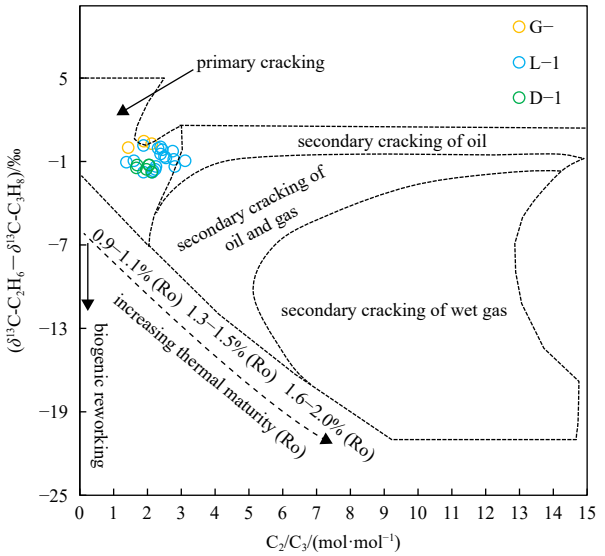

Fig. 5. The plot of ethane/propane (C_2/C_3) molar ratio versus δ^{13}C-C$_2$H$_6$–δ^{13}C-C$_3$H$_8$ (refer to Prinzhofer and Battani, 2003) showing the natural gases of the eastern Cote d'Ivoire Basin are dominated by primary cracking gases.

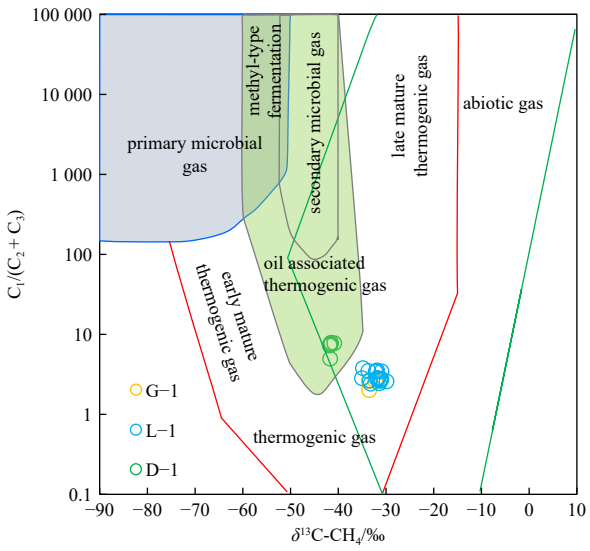

Fig. 6. Genetic diagram of δ^{13}C-CH$_4$ versus $C_1/(C_2+C_3)$ showing the genetic type of the natural gases in the eastern Cote d'Ivoire Basin. The boundary lines are from Milkov and Etiope (2018).

In Fig. 8, the typical oil-type gases of Well D-1 and some mixed-type gases of Well G-1 and Well L-1 are in a thermally mature stage, with Ro values of less than 1.3%. In addition, the relationship between natural gas $\delta^{13}C_1$ and equivalent vitrinite reflectance (VR_{eq}, $\delta^{13}C_1 = 25.55 \times \lg VR_{eq} - 40.76$) (Gang et al., 1997) was used to evaluate the maturity of oil-type gases in this study. The caculated VR_{eq} is between 0.96% and 1.0%. The other gas samples ($\delta^{13}C_2$ values less than –29‰) of Well L-1 and Well G-1 fall in a range of highly mature stage of sapropelic-type gas. This is inconsistent with no gas samples falling into the area of secondary cracking of oil and gas samples as indicated by Fig. 5, as well as their low dryness (0.65–0.77). In view of that $\delta^{13}C_1$

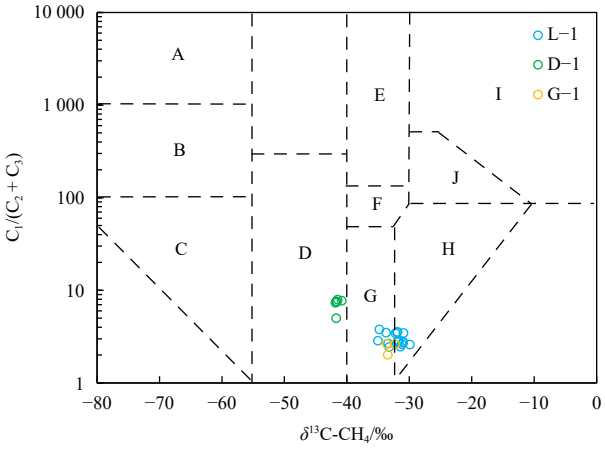

Fig. 7. The plot of δ^{13}C-CH$_4$ and $C_1/(C_2+C_3)$ distinguishing the genetic types of the natural gases in the eastern Cote d'Ivoire Basin. (A: biogenic gas; B: biogenic gas and sub-biogenic gas; C: sub-biogenic gas; D: oil-type gas; E: oil-type cracked gas; F: oil-type cracked gas and coal-derived gas; G: condensate oil-associated gas and coal-derived gas; H: coal-derived gas; I: inorganic gas; J: inorganic gas and coal-derived gas [plot after Dai 1992)].

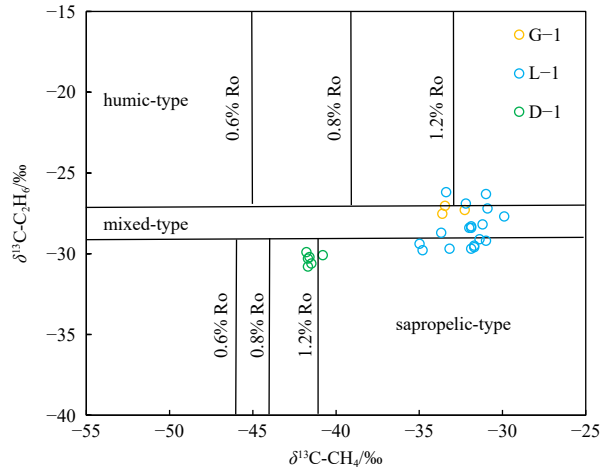

Fig. 8. The types and thermal maturity of natural gas classification diagram based on δ^{13}C-CH$_4$ and δ^{13}C-C_2H_6 data in the eastern Cote d'Ivoire Basin. The boundary lines are based on Dai (1992), Dai et al. (2005), and Li et al. (2022).

values of coal-derived gases are usually 7‰ to 8‰ higher than that of oil-type gases at the same thermal maturity stage (Dai et al., 1987; Dai et al., 2005), we propose that the gases of Well G-1 and Well L-1 falling in the high maturity zone is attributed to the notably higher $\delta^{13}C_1$ values, which is caused by the mixing of coal-derived gases and oil-associated gases in a mature stage (Ro generally varies from 1.0% to 1.3%) (Wu et al., 2020).

5.3 *Origins of natural gases*

The natural gases of three wells in the eastern Cote d'Ivoire Basin are mainly distributed in the Upper Albian sandstone reservoirs of delta facies. According to our studies on natural gas components and stable carbon isotopes, these gases were generated from the primary cracking of gas-prone and oil-prone kerogen, with Ro less than 1.3%. Combined with the types and thermal maturity of organic matter, we suggest that the transitional-to-marine source rocks during the Late Albian are the most likely hydrocarbon sources of the gas reservoirs.

Firstly, both sapropelic source rocks and humic source rocks developed during the late Albian. In the earliest stage of the Cretaceous separation of African and South American plates, restricted connection to the ocean and continuous marine transgression resulted in the continuous expansion of the restricted marine environment as well as the fining-upward deltaic sequence in nearshore zone (Pletsch et al., 2001). This can be also substantiated by the quality variation of the Upper Albain source rocks from the studied three wells: humic source rocks in delta facies mainly developed in the deep strata of the Upper Albian making them favourable for coal-derived gas generation, then sapropelic source rocks in lagoon facies with higher hydrocarbon generation potential developed in a wider range in the shallower strata (Fig. 9a). Therefore, the natural gases generated from the Upper Albian source rocks have the origins of both coal-derived and oil-type sources.

Secondly, basin modelling of the eastern Cote d'Ivoire Basin has been performed in previous research (Rüpke et al., 2010), indicating that the Upper Albian source rocks with moderate maturity (Ro less than 1.3%) were deposited in majority of the study area (Fig. 9b). Therefore, the oil-prone source rocks in the shallow strata are capable of generating oils. Several crude oil samples from Upper Albian reservoirs have been analyzed for oil-to-source correlation in the study area (report "Geochemical Solutions International, Inc. 2010. petroleum geochemistry of Vanco D-1 oil offshore Ghana"; report "Geochemical Solutions International, Inc. 2014. geochemical characterization of mud and headspace gas, sidewall core, cuttings, drilling mud and crude oil samples from Well L-1, Cape Three Points Deep Water Block Ghana"). These reports proposed a dominant contribution from lacustrine source rocks, but the lacustrine hydrocarbon supply horizon is unclear due to lack of samples and the corresponding geochemical data. In this study, we suggest a contribution from marine source rocks of the Upper Albian according to the similar biomarker characteristics between oils and mudstones of the Upper Albain (Fig. 10). Evidence includes abundant C_{30} 24-*n*-propyl steranes (marine precursors), the absence of oleanane, sterane/hopane ratio (oil: 0.31, mudstone: 0.34), gammacerane/hopane (oil: 0.15, mudstone: 0.14), C_{35}/C_{34} hopane (oil: 0.64, mudstone: 0.69), and similar maturity parameter values (e.g. Ts/Tm, $\alpha\beta\beta/(\alpha\alpha\alpha+\alpha\beta\beta)$ C_{29} sterane, and 20S/(20S + 20R) C_{29} $\alpha\alpha\alpha$-sterane). Combined with the down-hole variation of source rock quality (Fig. 9a), it is likely that the oil-type gases with moderate maturity of Well D-1 originates from the nearby oil-prone source rocks in the shallow layer of the Upper Albian.

For the mixed oil-type gases and coal-derived gases from Well G-1 and Well L-1, we propose that the *in situ* thick humic source rocks made a major contribution to the coal-derived gases. A small amount of oil-type gases might be derived from the nearby or downdip sapropelic source rocks of the Upper Albian. In addition, the oil-type gases likely escaped from a deeper oil pool and later mixed with the coal-derived gases in the Upper reservoirs.

6 Conclusions

The source rocks potential as well as molecular composition and stable carbon isotope composition of natural gases have

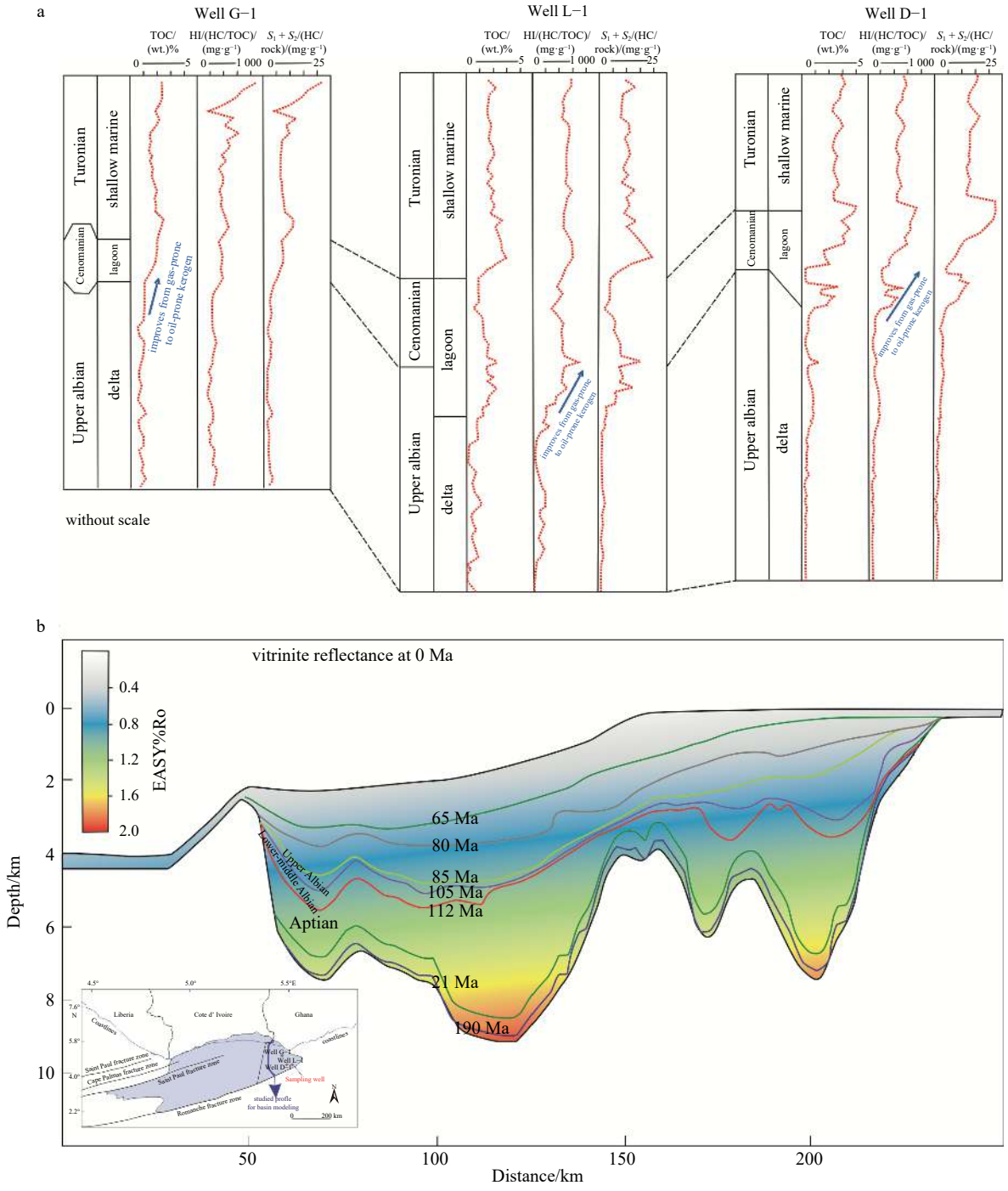

Fig. 9. Down-hole variation of source rock quality [total organic carbon (TOC), generation potential (S_1 + S_2), and hydrogen index (HI)] from Turonian to Upper Albain in the eastern Cote d'Ivoire Basin (a). Present temperature and maturity fields of the eastern Cote d'Ivoire Basin (modified from Rüpke et al., 2010) (b).

been comparatively studied. Based on the data from total organic content and Rock-Eval pyrolysis, both sapropelic source rocks and humic source rocks developed during the late Albian. The normal order of $\delta^{13}C_1 < \delta^{13}C_2 < \delta^{13}C_3$ and several cross-plots based on molecular composition and stable carbon isotopes (i.e. the plot based on $\delta^{13}C_1$, $\delta^{13}C_2$, and $\delta^{13}C_3$; the plot of (C_2/C_3) molar ratio versus $\delta^{13}C_6$-$\delta^{13}C_3$; the plot of $\delta^{13}C_1$ versus $C_1/(C_2+C_3)$) show that the natural gases in the eastern Cote d'Ivoire Basin originate from the primary cracking of kerogen. Natural gas samples were divided into two groups: oil-type gases from Well D-1; a mixed oil- type gases and coal-derived gases from Well G-1 and Well L-1. The plot of $\delta^{13}C_1$ versus $\delta^{13}C_2$ and the equivalent vitrinite reflectance (VR_{eq}) indicate that the gases are in a mature stage (Ro generally varies from 1.0% to 1.3%). Combined with the types and thermal maturity of organic matter, basin modelling, and oil-source correlation, we suggest that the transitional-to-marine source rocks during the late Albian made a great contribution to the coal-derived gases and oil-type gases.

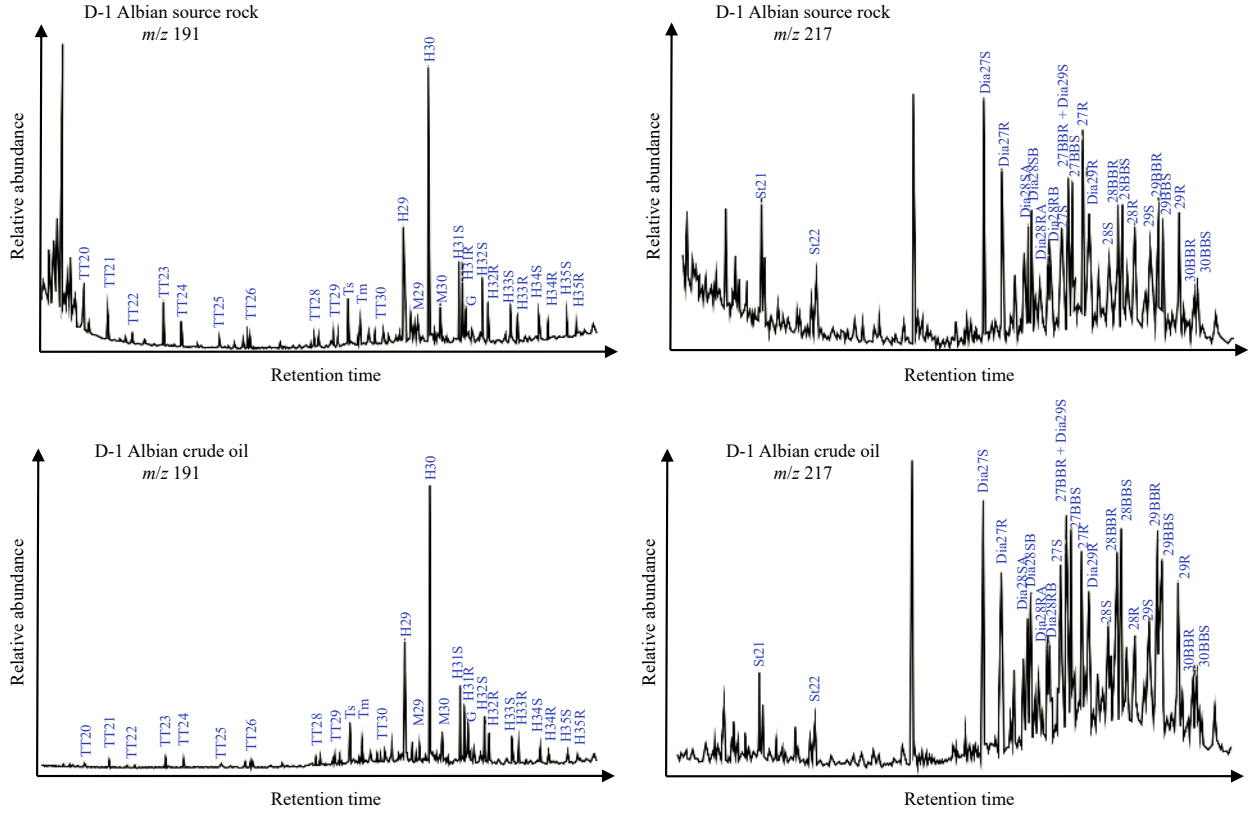

Abbreviation	Full name	Abbreviation	Full name
TT(20~30)	C_{20-30}Tricyclic terpane	Dia28SA	24-methyl-13β(H), 17α(H)-C28 diasterane (20S) a
Ts	18α(H)-C_{27}trisnorhopane	Dia28SB	24-methyl-13β(H), 17α(H)-C28 diasterane (20S) b
Tm	17α(H)-C_{27}trisnorhopane	Dia28RA	24-methyl-13β(H), 17α(H)-C28 diasterane (20R) a
H	hopane	Dia28RB	24-methyl-13β(H), 17α(H)-C28 diasterane (20R) b
M	moretane	27S	5α(H), 14α(H), 17α(H)-C27 sterane (20S)
H31S	17α(H),21β(H)-C_{31}hopane (22S)	27BBR + Dia29S	5α(H), 14α(H), 17α(H)-C27 sterane (20R)
H31R	17α(H),21β(H)-C_{31}hopane (22S)	27BBS	+ 24-ethyl-13β(H), 17α(H)-C29 diasterane (20S)
G	gammacerane	27R	5α(H),14β(H),17β(H)-C27 sterane (20S)
H32S	17α(H),21β(H)-C_{32}hopane (22S)	Dia29R	5α(H),14α(H),17α(H)-C27 sterane (20R)
H32R	17α(H),21β(H)-C_{32}hopane (22S)	28S	24-ethyl-13β(H),17α(H)-C29 diasterane (20S)
H33S	17α(H),21β(H)-C_{33}hopane (22S)	28BBR	24-methyl-5α(H),14α(H),17α(H)-C28 sterane (20S)
H33R	17α(H),21β(H)-C_{33}hopane (22S)	28BBS	24-methyl-5α(H),14β(H),17β(H)-C28 sterane (20R)
H34S	17α(H),21β(H)-C_{34}hopane (22S)	28R	24-methyl-5α(H),14β(H),17β(H)-C28 sterane (20S)
H34R	17α(H),21β(H)-C_{34}hopane (22S)	29S	24-methyl-5α(H),14α(H),17α(H)-C28 sterane (20R)
H35S	17α(H),21β(H)-C_{35}hopane (22S)	29BBR	24-ethyl-5α(H),14α(H),17α(H)-C28 sterane (20S)
H35R	17α(H),21β(H)-C_{35}hopane (22S)	29BBS	24-ethyl-5α(H),14β(H),17β(H)-C29 sterane (20R)
St21	pregnane	29R	24-ethyl-5α(H),14β(H),17β(H)-C29 sterane (20S)
St22	homopregnane	30BBR	24-ethyl-5α(H),14α(H),17α(H)-C29 sterane (20R)
Dia27S	13β(H), 17α(H)-C_{27} diasterane (20S)	30BBS	24-n-propyl-5α(H),14β(H),17β(H)-C30 sterane (20R)
Dia27R	13β(H), 17α(H)-C27 diasterane (20R)		24-n-propyl-5α(H),14β(H),17β(H)-C30 sterane (20S)

Fig. 10. Mass chromatograms (m/z 191 and m/z 217) of the Upper Albian source rock and crude oil from Well D-1 (data from preliminary report of Geochemical Solutions International, Inc).

References

Antobreh A A, Faleide J I, Tsikalas F, et al. 2009. Rift–shear architecture and tectonic development of the Ghana margin deduced from multichannel seismic reflection and potential field data. Marine and Petroleum Geology, 26(3): 345–368, doi: 10.1016/j.marpetgeo.2008.04.005

Atta-Peters D, Achaegakwo C A, Kwayisi D, et al. 2015. Palynofacies and source rock potential of the ST-7H well, offshore Tano Basin, western region, Ghana. Journal of Earth Science, 4(1): 1–20

Atta-Peters D, Garrey P. 2014. Source rock evaluation and hydrocarbon potential in the Tano Basin, south western Ghana, west Africa. International Journal of Oil, Gas and Coal Engineering, 2(5): 66–77

Basile C, Mascle J, Benkhelil J, et al. 1998. Geodynamic evolution of the Côte d'Ivoire-Ghana transform margin: an overview of Leg 159 results. In: Mascle J, Lohmann G P, Moullade M, eds. Proceedings of the Ocean Drilling Program, Scientific Results. 101–110 (doi:10.2973/odp.proc.sr.159.048.1998)

Basile C, Mascle J, Popoff M, et al. 1993. The Ivory Coast-Ghana transform margin: a marginal ridge structure deduced from seismic data. Tectonophysics, 222(1): 1–19, doi: 10.1016/0040-1951(93)90186-N

Bempong F K, Ozumba B M, Hotor V, et al. 2019. A review of the geology and the petroleum potential of the Cretaceous Tano Basin of Ghana. Journal of Petroleum & Environmental Biotechno-

logy, 10(4): 1000395
Benkhelil J, Mascle J, Guiraud M. 1998. Sedimentary and structural characteristics of the Cretaceous along the Côte d'Ivoire-Ghana transform margin and in the Benue Trough: a comparison. In: Mascle J, Lohmann G P, Moullade M, eds. Proceedings of the Ocean Drilling Program, Scientific Results. 93–99, doi: 10.2973/odp.proc.sr.159.007.1998
Bernard B B, Brooks J M, Sackett W M. 1976. Natural gas seepage in the Gulf of Mexico. Earth and Planetary Science Letters, 31(1): 48–54, doi: 10.1016/0012-821X(76)90095-9
Berner U, Faber E. 1996. Empirical carbon isotope/maturity relationships for gases from algal kerogens and terrigenous organic matter, based on dry, open-system pyrolysis. Organic Geochemistry, 24(10-11): 947–955, doi: 10.1016/S0146-6380(96)00090-3
Berner U, Faber E, Stahl W. 1992. Mathematical simulation of the carbon isotopic fractionation between huminitic coals and related methane. Chemical Geology: Isotope Geoscience Section, 94(4): 315–319, doi: 10.1016/0168-9622(92)90006-V
Bird S, Geno K, Enciso G. 2001. Potential deep water petroleum system, ivory coast, west Africa. In: Fillon R H, Rosen N C, Weimer P, et al, eds. Petroleum Systems of Deep-Water Basins–Global and Gulf of Mexico Experience. Tulsa: SEPM Society for Sedimentary Geology
Blarez E, Mascle J. 1988. Shallow structures and evolution of the Ivory Coast and Ghana transform margin. Marine and Petroleum Geology, 5(1): 54–64, doi: 10.1016/0264-8172(88)90039-6
Brownfield M E, Charpentier R R. 2006. Geology and total petroleum systems of the Gulf of Guinea province of west Africa. Reston: U. S. Geological Survey, 38
Chierici M A. 1996. Stratigraphy, palaeoenvironments and geological evolution of the Ivory Coast-Ghana Basin. In: Bulletin des Centres de Recherches Exploration-Production Elf-Aquitaine. Pau, France: Elf Aquitaine, 293–303
Clift P D, Lorenzo J, Carter A, et al. 1997. Transform tectonics and thermal rejuvenation on the Côte d'Ivoire–Ghana margin, west Africa. Journal of the Geological Society, 154(3): 483–489, doi: 10.1144/gsjgs.154.3.0483
Dai Jinxing. 1992. Identification of various genetic natural gases. China Offshore Oil and Gas (in Chinese), 6(1): 11–19
Dai Jinxing, Gong Deyu, Ni Yunyan, et al. 2014. Stable carbon isotopes of coal-derived gases sourced from the Mesozoic coal measures in China. Organic Geochemistry, 74: 123–142, doi: 10.1016/j.orggeochem.2014.04.002
Dai Jinxing, Ni Yunyan, Huang Shipeng, et al. 2016. Secondary origin of negative carbon isotopic series in natural gas. Journal of Natural Gas Geoscience, 1(1): 1–7, doi: 10.1016/j.jnggs.2016.02.002
Dai Jinxing, Ni Yunyan, Li Jian, et al. 2008. Carbon isotope types and significances of alkane gases from Junggar Basin and Tarim Basin. Xinjiang Petroleum Geology (in Chinese), 29(4): 403–410
Dai Jinxing, Qin Shengfei, Tao Shizhen, et al. 2005. Developing trends of natural gas industry and the significant progress on natural gas geological theories in China. Natural Gas Geoscience (in Chinese), 16(2): 127–142
Dai Jinxing, Wei Houfa, Song Yan, et al. 1987. Composition, carbon isotope characteristics and the origin of coal-bed gases in China and their implications. Science in China Series B, 30(12): 1324–1337
Dailly P, Henderson T, Hudgens E, et al. 2013. Exploration for Cretaceous stratigraphic traps in the Gulf of Guinea, west Africa and the discovery of the Jubilee Field: a play opening discovery in the Tano Basin, offshore Ghana. Geological Society, London, Special Publications, 369(1): 235–248
Davison I, Faull T, Greenhalgh J, et al. 2016. Transpressional structures and hydrocarbon potential along the Romanche fracture zone: a review. Geological Society, London, Special Publications, 431(1): 235–248
Espitalié J, Marquis F, Barsony I. 1984. Geochemical logging. In: Voorhees K J, ed. Analytical Pyrolysis. Amsterdam: Elsevier, 276–304
Faber E, Stahl W. 1984. Geochemical surface exploration for hydrocarbons in North Sea. AAPG Bulletin, 68(3): 363–386
Faramawy S, Zaki T, Sakr A A E. 2016. Natural gas origin, composition, and processing: a review. Journal of Natural Gas Science and Engineering, 34: 34–54, doi: 10.1016/j.jngse.2016.06.030
Gang Wenzhe, Gao Gang, Hao Shisheng. 1997. Carbon isotope of ethane applied in the analyses of genetic types of natural gas. Experimental Petroleum Geology (in Chinese), 19(2): 164–167
Garry P, Atta-Peters D, Achaegakwo C. 2016. Source - rock potential of the Lower Cretaceous sediments in SD - 1X well, offshore Tano Basin, south western Ghana. Petroleum and Coal, 58(4): 476–489
Hill R J, Jarvie D M, Zumberge J, et al. 2007. Oil and gas geochemistry and petroleum systems of the Fort Worth Basin. AAPG Bulletin, 91(4): 445–473, doi: 10.1306/11030606014
Huang Baojia, Huang Hao, Wang Zhenfeng, et al. 2015. Kinetics and model of gas generation of source rocks in the deepwater area, Qiongdongnan Basin. Acta Oceanologica Sinica, 34(4): 11–18, doi: 10.1007/s13131-015-0646-3
Lake Stuart, Derewetzky Aram, Frewin Neil. 2014. Structure, evolution, and petroleum systems of the Tano Basin, Ghana. In: Pindell J, Horn B, Rosen N, et al, eds. Sedimentary Basins: Origin, Depositional Histories, and Petroleum Systems. Houston: SEPM Society for Sedimentary Geology
Li Yong, Lu Jungang, Liu Xiangjun, et al. 2022. Geochemistry and origins of natural gas in the Hong-Che fault zone of the Junggar Basin, NW China. Journal of Petroleum Science and Engineering, 214: 110501, doi: 10.1016/j.petrol.2022.110501
Mascle J, Blarez E. 1987. Evidence for transform margin evolution from the Ivory Coast–Ghana continental margin. Nature, 326(6111): 378–381, doi: 10.1038/326378a0
Milkov A V. 2018. Secondary microbial gas. In: Wilkes H, ed. Hydrocarbons, Oils and Lipids: Diversity, Origin, Chemistry and Fate. Cham: Springer, 613–622
Milkov A V, Etiope G. 2018. Revised genetic diagrams for natural gases based on a global dataset of >20, 000 samples. Organic Geochemistry, 125: 109–120, doi: 10.1016/j.orggeochem.2018.09.002
Morrison J, Burgess C, Cornford C, et al. 2000. Hydrocarbon systems of the Abidjan margin. In: Offshore West Africa 2000, Conference and Exhibition. Abidjan, Cote d'Ivoire: Penn Well Publishing, 1–13
Pletsch T, Erbacher J, Holbourn A E L, et al. 2001. Cretaceous separation of Africa and south America: the view from the west African margin (ODP Leg 159). Journal of South American Earth Sciences, 14(2): 147–174, doi: 10.1016/S0895-9811(01)00020-7
Prinzhofer A, Battani A. 2003. Gas isotopes tracing: an important tool for hydrocarbons exploration. Oil & Gas Science and Technology, 58(2): 299–311
Prinzhofer A A, Huc A Y. 1995. Genetic and post-genetic molecular and isotopic fractionations in natural gases. Chemical Geology, 126(3-4): 281–290, doi: 10.1016/0009-2541(95)00123-9
Prinzhofer A, Mello M R, Takaki T. 2000. Geochemical characterization of natural gas: a physical multivariable approach and its applications in maturity and migration estimates. AAPG Bulletin, 84(8): 1152–1172
Prinzhofer A, Pernaton É. 1997. Isotopically light methane in natural gas: bacterial imprint or diffusive fractionation? Chemical Geology, 142(3–4): 193–200
Rooney M A, Claypool G E, Chung H M. 1995. Modeling thermogenic gas generation using carbon isotope ratios of natural gas hydrocarbons. Chemical Geology, 126(3-4): 219–232, doi: 10.1016/0009-2541(95)00119-0
Rüpke L H, Schmid D W, Hartz E H, et al. 2010. Basin modelling of a transform margin setting: structural, thermal and hydrocarbon evolution of the Tano Basin, Ghana. Petroleum Geoscience, 16(3): 283–298, doi: 10.1144/1354-079309-905
Strand K. 1998. Sedimentary facies and sediment composition changes in response to tectonics of the Côte d'Ivoire-Ghana transform margin. In: Mascle J, Lohmann G P, Moullade M, eds. Proceedings of the Ocean Drilling Program, Scientific Results. 113–123 (doi:10.2973/odp.proc.sr.159.009.1998)

Su Long, Zhang Dongwei, Yang Haizhang, et al. 2018. Chemical kinetics evaluation and its application of natural gas generation derived from the Yacheng formation in the deep-water area of the Qiongdongnan Basin, China. Acta Oceanologica Sinica, 37(1): 50–59., doi: 10.1007/s13131-018-1158-8

Tetteh J T. 2016. The Cretaceous play of Tano Basin, Ghana. International Journal of Applied Science and Technology, 6(1): 1–10

Wagner T. 2002. Late Cretaceous to Early Quaternary organic sedimentation in the eastern Equatorial Atlantic. Palaeogeography, Palaeoclimatology, Palaeoecology, 179(1–2): 113–147

Wang Zhenfeng, Sun Zhipeng, Zhang Daojun, et al. 2015. Geology and hydrocarbon accumulations in the deepwater of the northwestern South China Sea-with focus on natural gas. Acta Oceanologica Sinica, 34(10): 57–70, doi: 10.1007/s13131-015-0715-7

Whiticar M J, Suess E. 1990. Hydrothermal hydrocarbon gases in the sediments of the King George Basin, Bransfield Strait, Antarctica. Applied Geochemistry, 5(1–2): 135–147, doi: 10.1016/0883-2927(90)90044-6

Wu Xiaoqi, Liu Quanyou, Chen Yingbin, et al. 2020. Constraints of molecular and stable isotopic compositions on the origin of natural gas from Middle Triassic reservoirs in the Chuanxi large gas field, Sichuan Basin, SW China. Journal of Asian Earth Sciences, 204: 104589, doi: 10.1016/j.jseaes.2020.104589

Ye Jing, Rouby D, Chardon D, et al. 2019. Post-rift stratigraphic architectures along the African margin of the Equatorial Atlantic: part I the influence of extension obliquity. Tectonophysics, 753: 49–62, doi: 10.1016/j.tecto.2019.01.003